

## DRUMS OF HIGH WIDTH

ALEX DAVIES, PRATEEK GUPTA, SÉBASTIEN RACANIÈRE, GRZEGORZ SWIRSZCZ,  
ADAM ZSOLT WAGNER, THEOPHANE WEBER, AND GEORDIE WILLIAMSON

ABSTRACT. We provide a family of 5-dimensional prisms whose width grows linearly in the number of vertices. This provides a new infinite family of counter-examples to the Hirsch conjecture whose excess width grows linearly in the number of vertices, and answers a question of Matschke, Santos and Weibel.

### 1. INTRODUCTION

Let  $P$  be a convex polytope. The graph of  $P$  has nodes and edges corresponding to the vertices and edges of  $P$ . It is a fundamental unsolved problem to determine the diameter of this graph: how many steps does one need in order to walk between any two vertices, if one may only traverse edges.

This problem has deep connections to the complexity of the simplex method in linear programming. Indeed, lower bounds on the diameter of a polytope give lower bounds on the complexity of the simplex method. Determining the complexity of linear programming is one of Smale’s 18 problems, and is still unsolved.<sup>1</sup>

In 1957, Hirsch conjectured that the diameter of any convex polytope is bounded by  $n - d$ , where  $n$  is the number of facets and  $d$  is the dimension. This conjecture provides a simple linear bound for the diameter of a polytope, and would show that the diameter cannot provide a useful lower-bound for the complexity of the simplex method

In a breakthrough paper in 2011, Santos [San12] provided a counter-example to the Hirsch conjecture. His counter-example is in dimension 43 and has 86 facets, and the Hirsch bound fails by 1. Santos’ counter-example re-opens the door to the possibility that the diameter of polytopes might lead to interesting lower-bounds for the complexity of the simplex method.

Motivated by the “ $d$ -step theorem” of Klee and Walkup [KW67], Santos introduced the fundamental concept of a *drum*.<sup>2</sup> These are polytopes with two parallel facets containing all vertices. A remarkable theorem of Santos shows that interesting drums in small dimension (e.g. 5), may be used to construct interesting polytopes in high dimension (e.g. 43 in Santos’ famous example).

Experience suggests that the difficulty of gaining human understanding of polytopes grows exponentially in the dimension. This is one reason the drum concept is so useful—it allows one to compress high-dimensional difficulty into comparatively low dimension. More generally, the work of Santos and subsequent work of

---

GW is supported by ARC grant DP230102982.

<sup>1</sup>See [San12, §1] for some interesting history on the diameter of polytopes and its connection to the complexity of linear programming.

<sup>2</sup>*Drum* is our terminology, Santos called them *prismatoids*

Maschke, Santos and Weibel [MSW15] suggest that the study of drums may provide insights into the difficult question of the diameter of general polytopes.

Despite considerable interest in this problem, there remain very few examples of polytopes breaking the Hirsch bound. All known examples arise from interesting 5-dimensional drums. Such “non-Hirsch drums” appear to have remarkable structure, and are extremely rare. In [San12], Santos provides examples with enormous numbers of facets to show that the Hirsch conjecture can fail by any constant amount. More recently, Maschke, Santos and Weibel [MSW15] constructed more examples, showing that the excess width of drums (see below) can grow like the square root of the number of facets. In this paper we provide a family of 5-dimensional drums whose excess width grows linearly in the number of facets, answering a question posed in [MSW15]. Up to a constant factor, this is best possible. We are also able to uncover the mechanism leading to such examples.

**1.1. Main theorem.** As is often the case in the study of polytopes, it is useful to dualize. To a convex polytope  $P$  we may also associate its facet-ridge graph which has nodes given by the facets (=codimension 1 faces) of  $P$  and edges corresponding to ridges (=codimension 2 faces) of  $P$ . The facet-ridge graph of  $P$  agrees with the (vertex-edge) graph of the dual polytope. In this language the Hirsch conjecture states that the diameter of the facet-ridge of a convex polytope is bounded by  $n - d$  where  $n$  is the number of vertices of  $P$  and  $d$  is the dimension.

As discussed above, in this paper we consider *drums*. These are polytopes  $D$  that possess two fixed parallel facets  $D^-$  and  $D^+$  (the *drum skins*) which together contain all vertices of  $D$ . (For example, the cube and octahedron are both drums, with respect to any pair of opposite faces.) The width of a drum is the distance between the two drum skins in the facet-ridge graph. (Of course, the width of a drum provides a lower bound on the diameter of its facet-ridge graph.)

Santos explained how to start with a  $d$ -dimensional drum with  $n$  vertices of width  $\geq w$  and produce another drum with  $2(n - d)$  vertices in dimension  $n - d$  of diameter  $\geq w + n - 2d$ . Thus, the Hirsch conjecture implies that drums in dimension  $d$  have width at most  $d$ . Santos constructs his counter-example starting from a 5-dimensional drum with 48 vertices of width  $6 > 5$ .

More generally, Maschke, Santos and Weibel [MSW15] suggested that the study of the width of drums might provide insights on the diameter of general polytopes. Thus, one is led to consider the function

$$f_d(n) = \max_{d\text{-dimensional drums } D \text{ with } n\text{-vertices}} \text{width}(D) - d.$$

We call this function the *excess width*. The (disproved) Hirsch conjecture would have implied that this function is identically zero. All interesting examples so far involve 5-dimensional drums. The best results so far are due [MSW15] and show that  $f_5$  grows at least as fast as the square root of  $n$ .

Here we produce a new family of 5-dimensional drums  $D_k$  parametrized by  $k = 1, 2, \dots$ . They have  $16k + 24$  vertices. Our main theorem is:

**Theorem 1.1.**  $D_k$  has width  $\geq 5 + k$ .

Thus our results prove that  $f_5$  grows linearly in  $n$ . The question of whether this is possible was raised in [MSW15]. Note also that we hit (up to constants) the bounds established by [MSW15] for 5-dimensional drums<sup>3</sup>.

---

<sup>3</sup>Indeed, for any fixed constant  $d$ , the function  $f_d(n)$  is at most linear in  $n$ .

To translate this result back to the world of the Hirsch conjecture, Santos' Strong  $d$ -step theorem for spindles, which was mentioned above, implies the following:

**Corollary 1.2.** *For any integer  $k \geq 1$ , there exists a polytope  $P_k$  of dimension  $d = 16k + 19$  with  $2d$  facets, that has diameter at least  $d + k$ . That is, the Hirsch bound fails by  $k$ .*

In [San12, §6], Santos introduces the *Hirsch excess* of a (non-Hirsch) polytope which is defined as

$$\frac{\delta}{n-d} - 1$$

where  $\delta$  is its diameter,  $n$  the number of facets, and  $d$  the dimension. It is a useful measure of “how much” a polytope violates the Hirsch conjecture. One computes easily that the Hirsch excess of the polytopes arising from our family of drums is

$$\frac{k}{16k+19}$$

Thus, as  $k \rightarrow \infty$  the Hirsch excess of our family approaches  $1/16$ , which is the largest excess known (to the best of our knowledge).

**1.2. Symmetric search.** Our family of drums (given in §3) might seem arbitrary at first. Here we give some idea of how we discovered this family.

Let us first recall Santos' construction [San12] of his 5-dimensional drum of width 6, which he uses to produce the first counter-example to the Hirsch conjecture. Let  $\Gamma$  denote the finite group of orthogonal transformations of  $\mathbb{R}^5$  generated by the matrices

$$\begin{pmatrix} \pm 1 & 0 & 0 & 0 & 0 \\ 0 & \pm 1 & 0 & 0 & 0 \\ 0 & 0 & \pm 1 & 0 & 0 \\ 0 & 0 & 0 & \pm 1 & 0 \\ 0 & 0 & 0 & 0 & 1 \end{pmatrix} \quad \text{and} \quad \tau = \begin{pmatrix} 0 & 0 & 0 & 1 & 0 \\ 0 & 0 & 1 & 0 & 0 \\ 1 & 0 & 0 & 0 & 0 \\ 0 & 1 & 0 & 0 & 0 \\ 0 & 0 & 0 & 0 & -1 \end{pmatrix}.$$

Now, start with the five vectors

$$(1) \quad (18, 0, 0, 0, 1), (0, 0, 45, 0, 1), (15, 15, 0, 0, 1), (0, 0, 30, 30, 1), (10, 0, 0, 40, 1)$$

and consider all possible vectors obtained from one of these vectors by application of  $\Gamma$ . One obtains in this way 48 vectors, all of whose last coordinate is  $\pm 1$ . Hence, if  $D$  denotes the convex hull of these points then one obtains a drum with respect to the two faces  $D^-$  (resp.  $D^+$ ) where the last coordinate is  $-1$  (resp.  $+1$ ). Santos proves that  $D$  has width 6.

It is striking here that a rather complicated drum  $D$  is generated by a rather small *motif*, namely the list of vectors (1). We first tried random search over tuples of vectors whose entries are given by vectors whose entries are integers between 0 and 50.<sup>4</sup> Our first observation was that, although rare, we were able to find other width 6 drums in this way, which are genuinely different to Santos' construction. This is an illustration of an important principle in search problems, namely that searching for symmetric solutions is often better than brute-force (see e.g. [HW10]).

---

<sup>4</sup>More precisely, our search enforced some sparsity. We noticed the vectors in Santos' example have lots of zeros, and enforced this by first choosing a vanishing pattern (e.g.  $(A, 0, 0, 0, 1)$  or  $(A, 0, 0, B, 1)$ ) and then choosing entries for  $A, B$  etc.

Our second observation is that sampling entries of greatly differing scales was much more likely to produce counter-examples. For example, the motif

$$(2) \quad (0, 0, 3, 3, 1), (98, 0, 1, 0, 1), (100, 0, 0, 0, 1), (75, 75, 0, 0, 1).$$

generates a drum of width 6. (In fact, this is the first element of our family.) Note the differing scales here: the first two non-zero coordinates (e.g. 100, 98, 75) are of the order of 100, whereas the second two non-zero coordinates (1, 3) are of the order of 1. Random sampling with the first two coordinates “big” and the second two “small” appeared significantly more likely to produce drums of width 6.<sup>5</sup>

Our next step was to try to take a motif generating a drum of width  $k$ , and find a new motif by adding a single vector in order to produce a drum of width  $k + 1$ . This was performed by a combination of human and computer searches. After considerable effort, we found a family of motifs which led to drums of widths 8, 9, 10, all the way to 25. At this point we were confident that the construction worked, the proof only came later.

Interestingly, we found several examples of motifs which could be modified by the addition of additional vertices to produce drums of widths 6, 7, 8,  $\dots$ , however at some point it appeared impossible to add a single vector to increase the width. After considerable searches, the only family which produces widths  $5 + k$  for all  $k$  was the example of this paper.

*Remark 1.3.* This entire paper is simply the discussion of an interesting family of polytopes. We have not attempted to make the description of our polytopes as general as possible. We have simply found constants which do the job. The interested reader is encouraged to try to modify our constructions, or obtain constants which are the most general possible.

*Remark 1.4.* As we alluded to above, work on this paper relied heavily on extensive computations. Although we do not rely on any of the computations for the results of this paper, the interested reader may (like us) wish to experiment. For this reason we have prepared a colab [Co] which contains some basic functions to compute with the objects of this paper. Throughout the paper we include several remarks with pointers to computations and examples in the colab.

**1.3. Idea of the proof.** Each of our polytopes  $D_k$  is complicated, and we are unable to get a full description of their combinatorial structure. In order to prove that they have width  $\geq 5 + k$  we exploit a strategy developed in [San12, MSW15]. Namely, we obtain an explicit combinatorial description of the top and bottom drum skins (which are much simpler  $4d$  polytopes), and then try to glean as much as we can concerning their interaction. As in [San12, MSW15] we make heavy use of the symmetry group  $\Gamma$  to reduce computations.

A key tool developed in [San12] and extended in [MSW15] is that one may compute the width of a  $d$ -dimensional drum in terms of a topological data (a “pair of geodesic maps”) in the  $S^{d-2}$ -sphere. The pair of geodesic maps describes combinatorics of the interaction of the top and bottom drum skins. Then [MSW15, §2.1] explained how to distill out of this pair of geodesic maps a bipartite graph (the “incidence pattern”), whose nodes are the facets of the top and bottom drum skins.

---

<sup>5</sup>Drums of this form have a striking geometric form, which we refer to as a “double pancake”, see Remark 3.8.

They prove that the drum provides a counter-example to the Hirsch conjecture if and only if this graph is free of oriented 2-cycles [MSW15, Proposition 2.3].

We give a different point of view on the incidence pattern. We explain in §2.4 how one may compute it in terms of linear programming problems associated to the top and bottom drum skins. Roughly speaking, each facet of the top drum skin determines a linear programming problem on the bottom drum skin, and conversely. The solutions of these problems determines the incidence pattern. (We rename this map the “facet-vertex map”.)

Considerations of the incidence pattern makes it very believable that our drums are of width  $\geq 5 + k$ . However, this alone does not appear enough to conclude the proof. We conclude by a careful study of the interaction between ridges in the top drum skin and edges in the bottom drum skin.

**1.4. A comment on terminology.** In this work we call “drum” what Santos [San12] calls “prismatoid”. The reader may wonder why we decided to deviate from accepted nomenclature. We find the notation  $P$  (for a general *Polytope*) and  $D$  (for a *Drum*) natural and suggestive. We also find the terminology “drum” and “drum skin” evocative of the striking geometric structure.

**1.5. Acknowledgements.** We would like to thank the referees for their comments, which led to an improvement of this work.

## 2. DRUMS, SKINS AND WIDTHS

This is the theoretical foundation of this paper. We review some polytope basics and fix our notation. We then introduce the pair embedding and facet-vertex map, and explain how they can be used to bound the width of a drum from below.

**2.1. Conventions and notation for polytopes.** We work throughout with polytopes  $P$  within a  $d$ -dimensional affine space  $\mathbb{R}^d$ . *Polytope* means convex polytope.

We use *functional* throughout to mean affine linear functional. Recall that a *face* of a polytope  $P$  is a subset of the form  $\{p \in P \mid f(p) = 0\}$  for some functional  $f$  which is  $\geq 0$  on  $P$ . The dimension of a face is the dimension of its affine span.

By *facet*, *ridge*, *edge* and *vertex* we mean face of codimension 1, codimension 2, dimension 1 and dimension 0 faces respectively.

Given a polytope  $P$  with vertices  $v_1, \dots, v_m$  we will often abuse notation and identify a face  $F$  with the subset of vertices which it contains. Thus, “the edge  $\{v_1, v_2\}$ ” really means “the unique edge which contains  $v_1$  and  $v_2$ ”.

For any facet  $F$  there is a functional  $f_F$  which vanishes on  $F$  and is  $\geq 0$  on  $P$ . This functional (which is unique up to positive scalar) is the functional *defining*  $F$ .

Given a polytope  $P$ , a facet  $F$  and a point  $p$  outside  $P$  (i.e.  $p \notin P$ ) we say that  $p$  is *visible* from  $F$  if  $f_F(p) < 0$ . Intuitively,  $P$  is a piecewise linear (and opaque) planet, and we are a tiny being standing on the facet  $F$ . Visible points are all those points that we can see above the horizon of our planet.

Quite a few graphs come up in this paper. There is a conflict of terminology: vertices are often used to refer to the nodes of a graph, which might be e.g. facets of a polytope. In order to try to avoid becoming horribly confused we exclusively use *vertex* to refer to a 0-dimensional face of a polytope, and *node* to refer to the node of a graph.

**2.2. Conventions and notations for drums.** A *drum* is a polytope  $D$  with two distinguished parallel facets  $D^-$  and  $D^+$  which together contain all vertices of  $D$ . We often call  $D^-$  and  $D^+$  the *bottom* and *top drum skins*. (Thus, what we call a drum, Santos [San12, Definition 2.5] calls a *prismatoid*. In Santos' language, prismatoids are the polar duals of *spindles*. We will not need the language of spindles in this paper.)

As pointed out in [San12, §2.2], the requirement that the drum skins be parallel is not particularly important. One could instead require them simply to be disjoint, in which case a projective transformation can always be chosen to make them parallel.

Let us emphasise that the top and bottom drum skins are part of the data of a drum (i.e. a drum is a polytope  $D$ , together with two distinguished facets  $D^-$  and  $D^+$ ). For us, it will be convenient to always assume that our polytope is embedded in  $\mathbb{R}^d$  in such a way that the bottom and top drum skins are “at height  $-1$  and  $1$  respectively”. More precisely, if  $z$  denotes the last coordinate in  $\mathbb{R}^d$  we assume that

$$D^- = D \cap \{z = -1\} \quad \text{and} \quad D^+ = D \cap \{z = 1\}.$$

A drum is *simplicial* if all facets other than the drum skins are simplices. We make the following important assumption:

- (3) All drums considered in this paper are assumed simplicial.

*Remark 2.1.* One may understand simplicial polytopes are polytopes which are generic in their vertex description: any small perturbation of their vertices results in a combinatorially equivalent polytope. Similarly, one may understand simplicial drums as drums which are generic in their vertex description: any small perturbation of their vertices *preserving the drum skins* results in a combinatorially equivalent drum. Note that a simplicial drum is never a simplicial polytope unless its drum skins are simplices.

**2.3. The pair embedding.** In this section we provide a way to bound the width of a drum from below in terms of certain graphs associated to the top and bottom drum skins.

Consider a polytope  $P$ . We can associate two important graphs to  $P$ :

- (1) *The facet-ridge graph  $\mathcal{F}(P)$* : Nodes are facets of  $P$ , and two facets  $F$  and  $F'$  are joined if they have a ridge in common.
- (2) *The face graph  $\Delta(P)$* : Nodes are faces of  $P$  of any dimension. There is an edge between two nodes if they are incident and their dimension differs by 1. The face graph is graded by dimension of the face. We include the empty face, which has dimension  $-1$ .

Now consider a  $d$ -dimensional drum  $D$  with bottom drum skin  $D^-$  and top drum skin  $D^+$ . By definition, the *width* of  $D$  is

$$(4) \quad \text{width}(D) = \text{dist}_{\mathcal{F}(D)}(D^-, D^+).$$

(Here  $\text{dist}$  has the usual meaning in graph theory:  $\text{dist}(v, v) = 0$ ,  $\text{dist}(v, v') = 1$  if and only if  $v \neq v'$  and  $v$  and  $v'$  are incident etc.)

It makes things a little easier below to ignore the top and bottom drum skins, as they are of a very different character to the rest of the facets of the drum. The following definition only makes sense for drums:

- (1) *The trimmed facet-ridge graph  $\mathcal{F}^t(D)$* : The full subgraph of  $\mathcal{F}(D)$  consisting of facets  $\neq D^-, D^+$ .

Because of our assumption (3) we can grade  $\mathcal{F}^t(D)$  by dimension of the intersection of a facet with the top drum skin (which can take values  $0, 1, \dots, d-2$ ). We refer to this grading as the *height*, and denote it  $\text{ht } F$ . Because  $D^-$  (resp.  $D^+$ ) is incident to every facet at height 0 (resp.  $d-2$ ) we can rephrase the width in the trimmed facet-ridge graph as follows:

$$(5) \quad \text{width}(D) = \min_{\substack{F, F', \\ \text{ht } F=0, \text{ht } F'=d-2}} \text{dist}_{\mathcal{F}^t(D)}(F, F') + 2$$

Any facet  $F$  of  $D$  intersects the top and bottom drum skins  $D^-$  (resp.  $D^+$ ) in faces  $F_{\text{bot}}$  (resp.  $F_{\text{top}}$ ) of dimension  $a$  (resp.  $b$ ) with  $a + b = d - 2$ . The facet  $F$  is determined uniquely by  $F_{\text{bot}}$  and  $F_{\text{top}}$ . In this way we obtain an injection (a priori of sets):

$$\begin{aligned} \rho : \mathcal{F}^t(D) &\hookrightarrow \Delta(D^-) \times \Delta(D^+) \\ F &\mapsto (F_{\text{bot}}, F_{\text{top}}) \end{aligned}$$

This map will play a crucial role below. We call it the *pair embedding*.

Let us make the product  $\Delta(D^-) \times \Delta(D^+)$  into a graph via the (box) product: nodes are given by the Cartesian product of the nodes of  $\Delta(D^-)$  and  $\Delta(D^+)$  and  $(u_1, v_1)$  and  $(u_2, v_2)$  are connected by an edge if and only if either  $u_1 = u_2$  and  $v_1, v_2$  are incident, or  $u_1$  and  $u_2$  are incident and  $v_1 = v_2$ . The importance of the pair embedding is due to the following proposition, which bounds distance in the trimmed facet ridge graph in terms of the image under the pair embedding.

**Proposition 2.2.** *For any two faces  $F, F' \in \mathcal{F}^t(D)$  we have*

$$\text{dist}_{\mathcal{F}^t(D)}(F, F') \geq \frac{1}{2} \text{dist}_{\Delta(D^-) \times \Delta(D^+)}(\rho(F), \rho(F')).$$

*Proof.* Suppose that  $F, F'$  are incident faces in  $\mathcal{F}^t(D)$ . It is enough to show that the distance between  $\rho(F)$  and  $\rho(F')$  in  $\Delta(D^-) \times \Delta(D^+)$  is  $\leq 2$ .

For incident  $F, F'$  there are three possibilities:

- (1)  *$F$  and  $F'$  intersects  $D^+$  (equivalently  $D^-$ ) in faces of different dimensions.*  
In this case if

$$\rho(F) = (F_{\text{bot}}, F_{\text{top}}) \quad \text{and} \quad \rho(F') = (F'_{\text{bot}}, F'_{\text{top}})$$

then  $F_{\text{bot}}$  and  $F'_{\text{bot}}$  (resp.  $F_{\text{top}}, F'_{\text{top}}$ ) are incident in  $\Delta(D^-)$  (resp.  $\Delta(D^+)$ ).  
Hence

$$\text{dist}_{\Delta(D^-) \times \Delta(D^+)}(\rho(F), \rho(F')) = 2.$$

- (2)  *$F$  and  $F'$  have the same intersection with  $D^-$ .* In this case if

$$\rho(F) = (F_{\text{bot}}, F_{\text{top}}) \quad \text{and} \quad \rho(F') = (F'_{\text{bot}}, F'_{\text{top}})$$

then  $F_{\text{bot}} = F'_{\text{bot}}$ , and  $F_{\text{top}}$  and  $F'_{\text{top}}$  share a common codimension 1 face, and hence are of distance 2 in  $\Delta(D^+)$ .

- (3)  *$F$  and  $F'$  have the same intersection with  $D^+$ .* In this case if

$$\rho(F) = (F_{\text{bot}}, F_{\text{top}}) \quad \text{and} \quad \rho(F') = (F'_{\text{bot}}, F'_{\text{top}})$$

then  $F_{\text{top}} = F'_{\text{top}}$ , and  $F_{\text{bot}}$  and  $F'_{\text{bot}}$  share a common codimension 1 face, and hence are of distance 2 in  $\Delta(D^-)$ .

This completes the proof.  $\square$

Proposition 2.2 is not quite strong enough for our needs. We need a slight strengthening, which is obtained by observing that some facets of  $D^-$  and  $D^+$  never occur in the image of the pair embedding. More precisely, consider the full subgraphs with nodes

$$\begin{aligned}\Delta_D(D^+) &= \{F_{\text{top}} \mid F \text{ facet of } D\} \subset \Delta(D^+), \\ \Delta_D(D^-) &= \{F_{\text{bot}} \mid F \text{ facet of } D\} \subset \Delta(D^-).\end{aligned}$$

In other words, the nodes of  $\Delta_D(D^+)$  consists of all faces of  $D^+$  which occur as  $F_{\text{top}}$  for some facet  $F$  of  $D$ , and similarly for  $\Delta_D(D^-)$ .

Because the image of the pair embedding lands in the full subgraph

$$\Delta_D(D^-) \times \Delta_D(D^+) \subset \Delta(D^-) \times \Delta(D^+)$$

we have:

**Proposition 2.3.** *For any two faces  $F, F' \in \mathcal{F}^t(D)$  we have*

$$\text{dist}_{\mathcal{F}^t(D)}(F, F') \geq \frac{1}{2} \text{dist}_{\Delta_D(D^-) \times \Delta_D(D^+)}(\rho(F), \rho(F')).$$

**2.4. The facet-vertex map.** Consider the composition of the pair embedding with the projection

$$\mathcal{F}^t(D) \rightarrow \Delta(D^-) \times \Delta(D^+) \twoheadrightarrow \Delta(D^-).$$

Given a face  $F \in \Delta(D^-)$  it is difficult in general to decide whether it is in the image of this map, and if it is, in how many ways. (In the language of the previous section, deciding membership of  $\Delta_D(D^+)$  and  $\Delta_D(D^-)$  is complicated in general.)

However the situation simplifies significantly when  $F$  is a facet of  $D^-$ :

**Proposition 2.4.** *For any facet  $F$  of  $D^-$  there exists a unique vertex  $x_F$  of  $D^+$  such that  $(F, \{x_F\})$  is in the image of  $\rho$ .*

*Proof.* We first claim that any  $F$  facet of  $D^-$  is a ridge of the whole drum  $D$ . Indeed, take any functional  $f$  which is zero on  $F$  and  $> 0$  on  $D^-$ . If  $g$  is a functional which is zero on  $D^-$  and  $= 1$  on  $D^+$  then, for  $N$  large enough,  $f + Ng$  is  $\geq 0$  on  $D$  and zero exactly on  $F$ , which proves that  $F$  is a ridge.

In any polytope there are exactly two facets incident to any ridge. In the case of our ridge  $F$ , one such facet is  $D^-$ . The other facet (call it  $A$ ) intersects  $D^+$  in a single point  $x$  (by our simpliciality assumption (3)). This proves existence. To get uniqueness notice that any facet of  $D$  which intersects  $D^-$  in  $F$  is necessarily incident to  $F$ , and hence is equal to  $A$ , by the statement opening this paragraph.  $\square$

We call the resulting maps

$$\begin{aligned}\phi^- &: \text{facets of } D^- \rightarrow \text{vertices of } D^+ \\ \phi^+ &: \text{facets of } D^+ \rightarrow \text{vertices of } D^-\end{aligned}$$

the *facet-vertex maps*.

*Remark 2.5.* These maps (in a slightly different notation) play a key role in the 1970s counter-example to Hirsch in the unbounded setting [KW67].

*Remark 2.6.* One can use the facet-vertex maps to construct a bipartite graph with nodes given by the facets of  $D^+$  and  $D^-$ , and an edge from  $F \in D^+$  to  $F' \in D^-$  (resp.  $F' \in D^-$  to  $F \in D^+$ ) if  $\phi^+(F) \in F'$  (resp.  $\phi^-(F') \in F$ ). It is then easy to see from Proposition 2.2 that  $D$  is non-Hirsch (i.e. of width  $\geq d + 1$ ) if and only if the



resulting graph contains no oriented 2-cycles. This was first observed in [MSW15, Proposition 2.3] (the authors call the above graph the ‘‘incidence pattern’’). In our opinion, this observation provides the easiest way to check that Santos’ example is of width  $\geq 6$ .

**2.5. Determining the facet-vertex map.** There is a beautiful way to determine the facet-vertex maps. This is the method that we will use in practice below.

In order to describe this method, let us ignore the last coordinates and regard the top and bottom drum skins as embedded in the same affine space. Thus, if our drum  $D$  sits inside  $\mathbb{R}^d$ , we regard  $D^+$  and  $D^-$  as sitting inside the same  $\mathbb{R}^{d-1}$ , via the affine embeddings

$$(6) \quad \mathbb{R}^{d-1} \times \{1\} = \mathbb{R}^{d-1} = \mathbb{R}^{d-1} \times \{-1\}$$

(In other words, we ignore the last (‘‘drum’’) coordinate).

Now, for any facet  $F$  of  $D^+$  we can consider a defining functional  $f_F$ . (Recall that this means that  $f_F$  is  $\geq 0$  on  $D^+$  and is  $= 0$  on  $F$ .) We claim:

**Lemma 2.7.** *We have*

$$\phi^+(F) = v$$

where  $v$  is the vertex of  $D^-$  where  $f_F$  obtains its minimum value.

*Proof.* Consider the unique facet  $F' \neq D^+$  of  $D$  which contains  $F$ , and let  $f$  denote its defining functional. By definition,  $F'$  has a unique vertex not belonging to  $D^+$  and  $\phi^+(F) = v$ . Let us write  $f$  out in coordinates

$$f_+ : (x_1, \dots, x_d) \mapsto a_0 + \sum_{i=1}^d a_i x_d.$$

If we restrict  $f$  to  $\mathbb{R} \times \{1\}$  we get the functional

$$(7) \quad f_+ : (x_1, \dots, x_{d-1}) \mapsto a_0 + a_d + \sum_{i=1}^{d-1} a_i x_d.$$

Because  $f$  is zero on  $F'$  and  $\geq 0$  on  $D$ ,  $f_+$  is zero on  $F$  and  $> 0$  on  $D^+ - F$ . In other words,  $f_+$  is a defining functional for  $F \subset D^+$ . Thus  $f_+$  and  $f_F$  agree, up to positive scalar multiple.

If we restrict  $f$  to  $\mathbb{R} \times \{-1\}$  we get the functional

$$(8) \quad f_- : (x_1, \dots, x_{d-1}) \mapsto a_0 - a_d + \sum_{i=1}^{d-1} a_i x_d$$

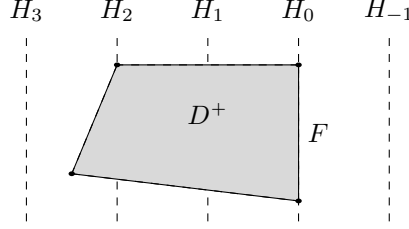
which is  $\geq 0$  on  $D^-$  and obtains its unique minimum value on  $D^-$  at  $v$ .<sup>6</sup> Hence  $f_+ + \lambda$  also obtains its minimum value on  $D^-$  at  $v$ , for any  $\lambda \in \mathbb{R}$ .

In particular,  $f_+ = f_- + 2a_d$  obtains its minimum at  $v$  and the lemma is proved.  $\square$

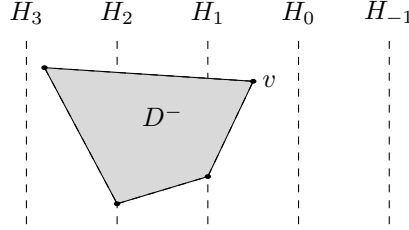
A more geometric way of formulating this is as follows. Consider first  $D^+$  and the fixed facet  $F$ . We can consider the family of parallel hyperplanes  $H_t$  given by  $f_F = t$  for  $t \in \mathbb{R}$ . For large values of  $t$ ,  $H_t$  does not intersect our polytope. As we increase  $t$  we get a family of parallel hyperplanes that eventually intersects  $D^+$  for

<sup>6</sup>This minimum value is of course 0, but we won’t need this.

small positive values of  $t$ . At  $t = 0$ ,  $H_t$  intersects  $D^+$  in  $F$ , and then  $H_t$  does not intersect  $D^+$  for any negative values of  $t$ :



Now let us keep our family of hyperplanes  $H_t$ , and instead focus on  $D^-$ . For very negative values of  $t$ ,  $H_t$  does not intersect  $D^-$ . As we increase  $t$  we get a family of hyperplanes getting closer and closer to  $D^-$ . Our simplicial assumption guarantees that the first time the hyperplanes  $H^t$  intersect  $D^-$ , the intersection will be in a single vertex  $\{v\}$ :



Then  $v$  is the image of our facet-vertex map:

$$\phi^+(F) = v.$$

*Remark 2.8.* Another way of thinking about this is the following: All facets in  $D^+$  determine linear programming problems on  $D^-$  whose solutions determine the facet-vertex map in one direction. Similarly, all facets of  $D^-$  determine linear programming problems on  $D^+$  whose solution determine the facet-vertex map in the other direction. This formulation of the two facet-vertex maps as “paired linear programs” seems attractive.

**2.6. Determining the pair embedding.** As in the previous section, we regard  $D^+$  and  $D^-$  as sitting inside the same  $\mathbb{R}^{d-1}$  via the identifications (of affine spaces)

$$(9) \quad \mathbb{R}^{d-1} \times \{1\} = \mathbb{R}^{d-1} = \mathbb{R}^{d-1} \times \{-1\}.$$

Suppose given a facet  $F^-$  of  $D^-$  of dimension  $d^-$  and a facet  $F^+$  of  $D^+$  of dimension  $d^+$ . We are interested in determining whether  $(F^-, F^+)$  is in the image of the pair embedding, and thus corresponds to a facet  $F$  of  $D$ . We have already seen that for this to be the case we must have

$$(10) \quad d^+ + d^- = d - 2.$$

The following provides an answer:

**Lemma 2.9.** *A pair  $(F^-, F^+)$  as above occurs in the image of the pair embedding if and only if there exists a functional  $f$  on  $\mathbb{R}^{d-1}$  whose minima on  $D^-$  (resp.  $D^+$ ) is equal to  $F^-$  (resp.  $F^+$ ).*

*Proof.* First suppose that such a functional  $f$  exists. The space of all functionals on  $\mathbb{R}^d$  which agree with  $f$  on  $\mathbb{R}^{d-1} \times \{-1\}$  is of dimension 1, and within this space we take the unique functional  $\tilde{f}$  which has the same value on  $F^-$  and  $F^+$ . By adding a constant, we can assume that  $\tilde{f}$  takes the value zero on  $F^-$  and  $F^+$ . Now  $\tilde{f}$  is  $\geq 0$  on  $D^-$  and  $D^+$  and hence is  $\geq 0$  on the whole drum  $D$ . The intersection of  $D$  with the set  $\tilde{f} = 0$  is a facet  $F$  containing  $F^-$  and  $F^+$ , by (10). Thus  $(F^-, F^+) = (F_{\text{bot}}, F_{\text{top}})$  as claimed.

On the other hand, consider a facet  $F$  of  $D$  which is not equal to  $D^-$  or  $D^+$ , and let  $F^- = F \cap D^-$  and  $F^+ = F \cap D^+$ . Let  $f_D$  be a defining functional for  $F$  and let  $f^-$  (resp.  $f^+$ ) denote its restriction to  $\mathbb{R}^{d-1} \times \{-1\}$  (resp.  $\mathbb{R}^{d-1} \times \{1\}$ ). Under the identifications (9), we have  $f^+ = f^- + \gamma$  for some constant  $\gamma$ . Thus the minimum of  $f^-$  on  $D^-$  (resp.  $D^+$ ) consists of  $F^-$  (resp.  $F^+$ ). In particular,  $f^-$  is our desired functional.  $\square$

This lemma has the following corollary, which will prove useful below:

**Corollary 2.10.** *Consider two facets  $F_1, F_2$  of  $D^+$  which intersect in a ridge  $R$ . If  $F_1$  and  $F_2$  map to the same vertex of  $D^-$  under the facet-vertex map, then the ridge  $R$  is not in the image of the pair embedding.*

*Proof.* Consider defining functionals  $f_1$  and  $f_2$  for  $F_1$  and  $F_2$ . Any positive linear combination  $\alpha f_1 + \beta f_2$  with  $\alpha, \beta > 0$  defines a functional vanishing on  $R$ , and all functionals vanishing on  $R$  and  $\geq 0$  on  $D^+$  are of this form. Now, observe that the minimum of  $\alpha f_1 + \beta f_2$  on  $D^-$  is always  $v$  for any  $\alpha, \beta > 0$ . Thus, there is no functional  $f$  which is zero on  $R$ ,  $\geq 0$  on  $D^+$  and has minimum on  $D^-$  consisting of anything but  $\{v\}$ . We conclude by the previous lemma.  $\square$

### 3. THE $+k$ FAMILY

In this section we introduce our  $+k$  family of drums, and study their geometry. First we give the definition, then we spend considerable time getting an explicit description of the top and bottom drum skins. We then compute the facet-vertex map, and hence obtain some basic knowledge of the pair embedding. We then use this to establish that they are of width  $\geq 5 + k$ .

**3.1. Definition.** Fix  $k \geq 1$ . We consider the following points in  $\mathbb{R}^5$ :

$$\begin{aligned} m_{\pm, \pm} &= (0, 0, \pm 3, \pm 3, 1) \\ p_{\pm} &= (98, 0, \pm 1, 0, 1) \\ a_1 &= (100, 0, 0, 0, 1) \\ a_2 &= (x_2, y_2, 0, 0, 1) \\ &\vdots \\ a_k &= (x_k, y_k, 0, 0, 1) \\ a_{k+1} &= (75, 75, 0, 0, 1) \end{aligned}$$

We denote the set of these points  $\{m_{\pm\pm}, p_{\pm}, a_i\}$ .

*Remark 3.1.* (1) We will be more precise about the  $a_i$  in a moment.

(2) Really  $m_{\pm\pm}$  is shorthand for 4 points. For example,

$$m_{+-} = (0, 0, +3, -3, 1).$$

Similarly,  $p_{\pm}$  is shorthand for 2 points, for example

$$p_+ = (98, 0, 1, 0, 1).$$

In order to define our drum, we use a group of symmetries to enlarge our set of points. Let

$$\varepsilon_i = \text{sign change at } i^{\text{th}} \text{ coordinate.}$$

So for example,  $\varepsilon_2 a_{k+1} = (75, -75, 0, 0, 1)$ . Let  $\tau'$  denote the permutation of the coordinates induced by  $(3, 4, 2, 1, 5)$ . Thus, for example,  $\tau' p_- = (0, -1, 98, 0, 1)$ . Now define

$$\tau = \varepsilon_5 \tau'.$$

Thus,  $\tau$  permutes the first 4 coordinates and flips the sign of the last coordinate. Note that  $\tau^2$  is the permutation of the coordinates induced by  $(2, 1, 4, 3)$ . Finally, consider the group:

$$\Gamma = \langle \tau, \varepsilon_i \mid 1 \leq i \leq 4 \rangle.$$

Note that  $\langle \varepsilon_i \mid 1 \leq i \leq 4 \rangle$  is a normal subgroup of  $\Gamma$  with quotient isomorphic to  $\mathbb{Z}/4\mathbb{Z}$ . In particular

$$(11) \quad |\Gamma| = 64.$$

We now define:

$$D_k = \text{convex hull of } \{g(v) \mid v \in \{m_{\pm\pm}, p_{\pm}, a_i\} \text{ and } g \in \Gamma\}$$

By construction,  $D_k$  is invariant under  $\Gamma$ . We will use this extensively below to simplify computations.

Also note that  $\tau$  exchanges top and bottom drum skins, and thus its square

$$\sigma = \tau^2$$

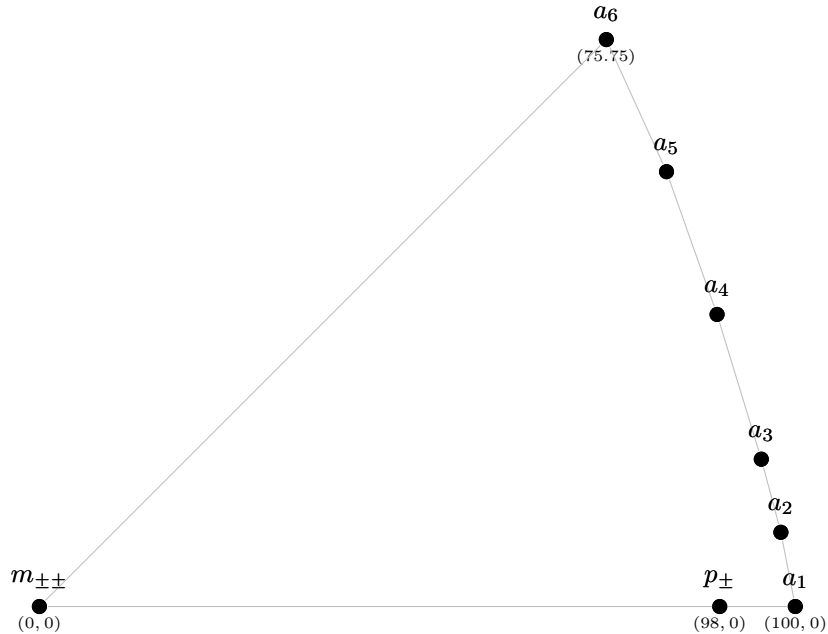
preserves the top and bottom drum skins. In particular, top and bottom drum skins are invariant under the subgroup

$$\Gamma^+ = \langle \sigma, \varepsilon_i \mid 1 \leq i \leq 4 \rangle \subset \Gamma.$$

In fact, it is easy to see that  $\Gamma^+$  is precisely the subgroup of  $\Gamma$  which stabilizes the top and bottom drum skins setwise.

*Remark 3.2.* The idea to consider drums which are symmetric under sign flips and a permutation is due to Santos [San12]. His counter-example to the Hirsch conjecture is of this form. Note that, up to permutation of any of the first four coordinates we could replace  $(3, 4, 2, 1)$  by any conjugate in  $S_4$ . Thus the important feature of  $\tau$  is that it is an 4-cycle.

*Remark 3.3.* Our permutation is determined by `MAIN_SYMMETRY` in the colab [Co], up to inversion and conversion to python indexing:  $1 \mapsto 0, 2 \mapsto 1, \dots$ . The transformation  $\tau$  is given by the function `permute_axes`.

FIGURE 1. Our points  $m_{\pm\pm}$ ,  $p_{\pm}$  and  $a_i$  for  $k = 5$ . (Not to scale!)

**3.2. Critical assumptions.** We now make explicit our assumptions on the points  $a_1, a_2, \dots, a_{k+1}$ . In picturing the points  $\{m_{\pm\pm}, p_{\pm}, a_i\}$  it is useful to ignore the last coordinate (which is always 1) and project to the first two coordinates. When we do so, we get a picture as in Figure 1. Note that all points in this figure are uniquely determined by their images in the projection with the exception of the image of  $m_{++}$  (which has the four points  $m_{\pm\pm}$  in its preimage) and the image of  $p_+$  (which has the two points  $p_{\pm}$  its preimage).

We have drawn the points in Figure 1 to try to illustrate our key assumptions. Our first is that our points lie in the first quadrant below the line  $y = x$ :

$$(12) \quad 100 = x_1 > x_2 > \dots > x_k > x_{k+1} = 75 \quad \text{and}$$

$$(13) \quad 0 = y_1 < y_2 < \dots < y_k < y_{k+1} = 75.$$

Our second is a simple convexity assumption:

$$(14) \quad \begin{array}{l} \text{The points } a_1, a_2 \dots a_{k+1} \text{ are in convex position,} \\ \text{i.e., no } a_j \text{ is in the convex hull of the other } a_i. \end{array}$$

Our third assumption says that the points  $a_i$  “almost lie on a line”:

$$(15) \quad \begin{array}{l} \text{For all } 1 \leq i \leq k, \text{ the line drawn through } a_i \text{ and } a_{i+1} \\ \text{meets the } x \text{ axis at } u, \text{ where } 100 \leq u \leq 102. \end{array}$$

It is clear that we can always choose  $k + 1$  points  $a_i$  satisfying (15).

The following elementary consequence of our assumptions will be important later.

**Lemma 3.4.** *The line drawn through  $a_i$  and  $a_{i+1}$  meets the  $y$  axis at  $v_i$ , where*

$$(16) \quad v_i \geq \frac{75}{1 - 75/102} > 283$$

*Remark 3.5.* The reader is reminded of Remark 1.3 when trying to make sense of constants!

*Proof.* Consider the lines  $L_i$  drawn through  $a_i$  and  $a_{i+1}$  for  $1 \leq i \leq k$ . Let  $u_i$  (resp.  $v_i$ ) denote the intersection point of  $L_i$  with the  $x$ -axis (resp.  $y$ -axis). By our convexity assumption (14) we have:

$$(17) \quad v_1 > v_2 > \cdots > v_k$$

By our convexity assumption (14) and our “almost on a line” assumption (15) we have:

$$(18) \quad u_1 < u_2 < \cdots < u_k \leq 102.$$

It follows (again by convexity) that if we consider the line  $L$  through  $a_{k+1} = (75, 75)$  and  $(102, 0)$  it meets the  $y$  axis at a point  $u$  satisfying

$$v_k > u.$$

Now an explicit computation yields that

$$u = \frac{75}{1 - 75/102}$$

and the lemma follows.  $\square$

Finally, we count the vertices of  $D_k$ , justifying the count in the introduction:

**Lemma 3.6.**  $D_k$  has  $16k + 24$  vertices.

*Proof.* The reader may easily check that our assumptions guarantee that any point in the  $\Gamma$  orbit of  $m_{\pm, \pm}$ ,  $p_{\pm}$  is indeed a vertex of  $D_k$ . We count the number of these orbits by exploiting the  $\Gamma$ -action and the orbit stabilizer theorem. Also note that up to the  $\Gamma$ -action we only need to consider  $m_{++}$ ,  $p_+$  and the  $a_i$  for  $1 \leq i \leq k + 1$ .

The stabilizer of  $m_{++}$  is  $\langle \varepsilon_1, \varepsilon_2, \tau^2 \rangle$ , and hence its orbit has size 8. Similarly the orbit of  $a_{k+1}$  has size 8. For  $a_1$  the stabilizer is  $\langle \varepsilon_2, \varepsilon_3, \varepsilon_4 \rangle$  and so its orbit also has size 8. The stabilizer of  $p_+$  is  $\langle \varepsilon_2, \varepsilon_4 \rangle$  and hence its orbit is of size 16. Finally, for  $a_i = (x_i, y_i, 0, 0, 1)$  for  $2 \leq i \leq k$  our assumptions (12) and (13) guarantee that  $x_i, y_i > 0$  and  $x_i \neq y_i$ ; hence its stabilizer is  $\langle \varepsilon_3, \varepsilon_4 \rangle$  and its orbit is of size 16.

Adding up we get

$$8 + 8 + 8 + 16 + (k - 1)16 = 16k + 24$$

as claimed.  $\square$

**3.3. The top drum skin.** It seems hopeless to study  $D_k$  in detail. However we can get a detailed understanding of the top drum skin  $D_k^+$ , which is what we do here.

By abuse of notation, we use the same notation as earlier for certain vertices of  $D_k^+$ :

$$\begin{aligned}
m_{\pm,\pm} &= (0, 0, \pm 3, \pm 3) \\
p_{\pm} &= (98, 0, \pm 1, 0) \\
a_1 &= (100, 0, 0, 0) \\
a_2 &= (x_2, y_2, 0, 0) \\
&\vdots \\
a_k &= (x_{k-1}, y_{k-1}, 0, 0) \\
a_{k+1} &= (75, 75, 0, 0)
\end{aligned}$$

One checks easily that all vertices of  $D_k^+$  are obtained from these vertices by acting by the group  $\Gamma^+$  generated by the permutation (12)(34) of coordinates together with all sign flips.

*Remark 3.7.* As described in the introduction, the motivation for this construction was Santos' original counterexample, which was the closure of the five points

$$(18, 0, 0, 0, 1), (0, 0, 45, 0, 1), (15, 15, 0, 0, 1), (0, 0, 30, 30, 1), (10, 0, 0, 40, 1)$$

under  $\Gamma$ . We started with this construction and experimented with adding points to the fundamental domain so that the width increases, until we eventually found a pattern that generalizes.

*Remark 3.8.* One aspect of the geometry of  $D$  is worth pointing out, namely its curious “double pancake” structure. Consider a pancake embedded in  $\mathbb{R}^3$  so that it is symmetric about the origin in the  $x$  and  $y$  coordinates. Points on the edge of the pancake have large  $x$  and  $y$  coordinates, and all points of the pancake have small  $z$  coordinates. One can imagine a  $4d$  version of this, (a “ $4d$  pancake”) with two large coordinates, and two small coordinates.

It is remarkable that in our example the top and bottom drum skins are both such  $4d$  pancakes:  $D^+$  has large first two coordinates (on the order of 100) and small second two coordinates (on the order of 1). The large and small coordinates are swapped in  $D^-$ . The reader wishing to see this structure more explicitly is referred to the cells “Understanding the top drum skin” and “The pancake structure” in the colab [Co].

It is also interesting to note that amongst our symmetric searches, those drums which exhibited the “double pancake” structure were much more likely to provide drums of large width. (See [MSW15, Lemma 2.13] and Remark 3.18.)

**3.4. Facets in the top drum skin.** Recall that our first goal is to come to grips with the top drum skin. The following is the first significant step towards the proof of our main theorem:

**Proposition 3.9.** *Every facet of  $D_k^+$  is conjugate under  $\Gamma^+$  to one of the following facets (for  $1 \leq i \leq k$ ):*

$$\begin{aligned}
B &= \{m_{++}, m_{+-}, p_+, a_{k+1}\}, \\
E_i &= \{m_{++}, m_{-+}, a_i, a_{i+1}\}, \\
C_i &= \{m_{++}, p_+, a_i, a_{i+1}\}.
\end{aligned}$$

*Remark 3.10.* The reader is referred to Figures 2, 3 and 4 which depict the projections of these 3 types of facets.

Our proof is in two steps:

- (1) We prove that the listed facets are indeed facets. To do this, we produce a functional which is zero on the specified vertices, and  $> 0$  on all other vertices of  $D_k^+$ .
- (2) We prove that we have all facets on our list up to  $\Gamma^+$  conjugacy. For this we check that all facets incident to a facet on our list are  $\Gamma^+$ -conjugates of facets on our list.

Actually, the second step gives us slightly more, namely good control of the incidence between the facets in the top drum skin. We exploit this fact in the next section.

*Proof that the claimed facets are facets:* Now, we roll up our sleeves. We handle each family of facets separately:

*Facet B:* Consider the functional given by the row vector:

$$f_B = \left(-1, -\frac{24}{25}, -49, 0, 3 \cdot 49\right)$$

One checks easily that  $f_B$  vanishes at  $m_{+,\pm}$ ,  $p_+$  and  $a_{k+1}$ . Furthermore,

- (1)  $f_B$  is  $> 0$  on  $m_{-,+}, m_{-,-}$ .
- (2)  $f_B$  is  $> 0$  on all points of the  $\Gamma^+$  orbit of  $p_+$  except  $p_+$ .

In order to establish that  $f_B$  is  $> 0$  on the  $\Gamma^+$  orbits of  $a_1, a_2, \dots, a_k$  we use a convexity argument. Consider the restriction of  $f_B$  to the plane  $(*, *, 0, 0)$ . It is given by the functional

$$-x - \frac{24}{25}y + 3 \cdot 49.$$

It is now easy to check that this functional is  $\geq 0$  on the convex hull of the  $\Gamma^+$ -orbits  $a_1, a_2, \dots, a_{k+1}$  and has a unique zero at  $a_{k+1}$ . Hence  $B$  is a facet as claimed.

*Facet  $E_i$ .* Let us view  $\mathbb{R}^4$  as the direct sum of vector spaces  $V_1 \oplus V_2$ , where  $V_1$  (resp.  $V_2$ ) is the subspace corresponding to the first and second (resp. third and fourth) coordinates. Note that the  $a_i$  lie in  $V_1$  and the  $m_{\pm\pm}$  lie in  $V_2$ . Consider *linear* functionals on  $V_1$  and  $V_2$  respectively defined as follows:

- (1)  $f_1$  is  $-1$  on  $a_i$  and  $a_{i+1}$  (and hence  $> -1$  at all other points in the  $\Gamma^+$ -orbit of the  $a_i$ 's);
- (2)  $f_2$  is  $-1$  on  $m_{++}$  and  $m_{-+}$  (and hence  $> -1$  on  $m_{-+}$  and  $m_{--}$ ).

Now consider the functional  $f = f_1 + f_2 + 1$  defined on  $\mathbb{R}^4$ . By property (1),  $f$  is  $\geq 0$  on the  $\Gamma^+$ -orbit of the  $a_i$  and  $= 0$  only at  $a_i$  and  $a_{i+1}$ . By property (2), it is zero on  $m_{++}$  and  $m_{-+}$  and  $> 0$  on  $m_{-+}$  and  $m_{--}$ .

It remains to check that  $f$  is  $> 0$  on the  $\Gamma^+$ -orbit of  $p_+$ . Firstly, note that  $f_2((c, d)) = -\frac{1}{3}d$  and hence  $f((\pm 98, 0, \pm 1, 0)) > 0$ . Also, amongst points of the form  $(0, \pm 98, 0, \pm 1)$ ,  $f$  achieves its minimum at  $(0, 98, 0, 1)$  by inspection. Hence we are done if we can show that

$$(19) \quad f_1((0, 98)) + f_2((0, 1)) > -1.$$

By our formula for  $f_2$ , we have  $f_2((0, 1)) = -\frac{1}{3}$ . Now, consider the line through  $a_i$  and  $a_{i+1}$  as in §3.2. We know that  $f$  takes the value  $-1$  along this line, and hence,



denoting by  $v$  the intersection point of this line with the  $y$ -axis,  $f_1((0, v)) = -1$ . Hence

$$f_1((0, 98)) = 98 \cdot f_1((0, 1)) = \frac{98}{v} f_1((0, v)) = -\frac{98}{v} > -\frac{98}{283},$$

where we have used (16) for the last inequality. Hence we have (19) and  $E_i$  is a facet as claimed.

*Facet  $C_i$ :* The points  $m_{++}, p_+, a_i, a_{i+1}$  are clearly affinely independent, and hence there exists a functional  $f$  which is  $= 0$  on these four points, and  $> 0$  at 0.

More precisely,  $f$  is defined up to a positive scalar. Hence, altering  $f$  if necessary, we may assume that  $f = f' + 1$  where  $f'$  is linear. Let us further decompose  $f$  as  $f = f_1 + f_2 + 1$  where  $f_1$  (resp.  $f_2$ ) is a linear functional on the first two (resp. second two) coordinates in the decomposition  $\mathbb{R}^4 = \mathbb{R}^2 \oplus \mathbb{R}^2$  that we used above. We know that:

- (1)  $f_1$  takes the value  $-1$  at  $a_i$  and  $a_{i+1}$  (because  $f$  vanishes at  $a_i, a_{i+1}$ );
- (2)  $f_2$  takes the value  $-1$  at  $(3, 3)$  (because  $f$  vanishes at  $m_{++} = (0, 0, 3, 3)$ ).

We still have to use the fact that  $f$  vanishes at  $p_+$ . In order to do so set

$$\delta_1 = f_1((98, 0)) \quad \text{and} \quad \delta_2 = f_2((1, 0)).$$

Because  $f(p_+) = f_1((98, 0)) + f_2((1, 0)) + 1 = 0$  we have

$$(20) \quad \delta_1 + \delta_2 = -1.$$

Now let  $u$  be defined such that  $f_1((u, 0)) = -1$ . (In other words,  $u$  is the intersection point of the line through  $a_i$  and  $a_{i+1}$  and the  $x$ -axis, considered in §3.2.) Because

$$-1 = f_1((u, 0)) = u f_1((1, 0)) = \frac{u}{98} \delta_1$$

we arrive at

$$(21) \quad \delta_1 = -\frac{98}{u}.$$

Note that our fundamental assumption (15) yields that  $100 \leq u \leq 102$  and hence that

$$-0.98 \leq \delta_1 < -0.96$$

(We have approximated by real numbers which will give us bounds sufficient for our needs. There is some wiggle room here.) In particular, using (20) we deduce that

$$-0.04 < \delta_2 \leq -0.02$$

Finally, if we write  $f_2 = (\alpha, \beta)$  then  $f_2((3, 3)) = -1$  gives the equation

$$(22) \quad \alpha + \beta = -\frac{1}{3}$$

and  $f_2((1, 0)) = \delta_2$  yields  $\alpha = \delta_2$ . Hence

$$(23) \quad f_2 = (\delta_2, -\frac{1}{3} - \delta_2).$$

Thus,  $f_2$  achieves its minimum ( $= -1$ ) on the set  $\{m_{++}, \dots, m_{--}\}$  at  $m_{++} = (3, 3)$ . This shows that  $f$  is  $> 0$  on  $m_{-+}, m_{+-}, m_{--}$ . (Alternatively, this follows directly from (23).) Similarly, using the definition of  $f_1$ , we see that  $f$  is  $\geq 0$  on the entire  $\Gamma^+$  orbit of the  $\{a_j\}$ , and is  $= 0$  only at  $a_i$  and  $a_{i+1}$ .

It remains to see that  $f$  is  $\geq 0$  on the  $\Gamma^+$ -orbit of  $p_+$ . We have already seen that  $f$  is zero on  $p_+$  and it is easy to see that it is then necessarily  $> 0$  on  $(98, 0, -1, 0)$  and  $(-98, 0, \pm 1, 0)$ . It is also immediate that among points of the form

$$(0, \pm 98, 0, \pm 1)$$

$f$  takes its minimal value at  $\sigma(p_+) = (0, 98, 0, 1)$ . Thus we are done if we can establish that

$$(24) \quad f_1((0, 98)) + f_2((0, 1)) > -1.$$

By (23) we have  $f_2((0, 1)) = -\frac{1}{3} - \delta_2$  and this quantity is  $> -1/3$ . Also, writing  $v$  for the intersection point of the line joining  $a_i$  and  $a_{i+1}$  with the  $y$ -axis (as in §3.2) we deduce that  $f_1((0, 98)) > -98/283$  using (16). Thus we have established (24) and  $C_i$  is a facet as claimed.  $\square$

*Proof that we have all facets:* We now proceed to the second half of the proof, namely proving that we have written down all facets of  $D_k^+$ . Note that all facets of  $D_k^+$  are 3-simplices, and hence have four neighbours in the facet ridge graph. It is enough to check that all four neighbours of each facet on our list are  $\Gamma^+$ -conjugates of facets on our list.

Consider the following diagram, which shows “obvious” incidences between facets:

$$(25) \quad \begin{array}{ccc} & & B \\ & & | \\ E_k & \text{-----} & C_k \\ | & & | \\ E_{k-1} & \text{-----} & C_{k-1} \\ | & & | \\ \vdots & & \vdots \\ | & & | \\ E_2 & \text{-----} & C_2 \\ | & & | \\ E_1 & \text{-----} & C_1 \end{array}$$

For example,  $E_i$  and  $E_{i+1}$  are incident because they share the three vertices  $m_{++}$ ,  $m_{+-}$  and  $a_{i+1}$ . Similarly,  $E_i$  and  $E_{i+1}$  share the three vertices  $m_{++}$ ,  $a_i$  and  $a_{i+1}$ .

We know that every facet is incident to 4 other facets (as  $D_k^+$  is 4-dimensional). Thus it is enough to complete this graph by showing that every facet above is incident to 4 facets, all of which are in the  $\Gamma^+$ -orbit of one of the facets above. (In other words, it remains to complete the above graph by giving the remaining “non-obvious” incidences, involving  $\Gamma^+$ -conjugates).

It is a straightforward check to see that around all facets  $\neq B$  we get the following graph:

$$(26) \quad \begin{array}{ccccccc} & & \sigma B & & B & & \\ & & | & & | & & \\ \epsilon_3 C_k & \text{---} & E_k & \text{---} & C_k & \text{---} & \epsilon_4 C_k \\ & & | & & | & & \\ \epsilon_3 C_{k-1} & \text{---} & E_{k-1} & \text{---} & C_{k-1} & \text{---} & \epsilon_4 C_{k-1} \\ & & | & & | & & \\ & & \vdots & & \vdots & & \\ & & | & & | & & \\ \epsilon_3 C_2 & \text{---} & E_2 & \text{---} & C_2 & \text{---} & \epsilon_4 C_2 \\ & & | & & | & & \\ \epsilon_3 C_1 & \text{---} & E_1 & \text{---} & C_1 & \text{---} & \epsilon_4 C_1 \\ & & | & & | & & \\ & & \epsilon_2 E_1 & & \epsilon_2 C_1 & & \end{array}$$

(One just needs to check that all edges represent genuine incidences between facets. In other words, that for every pair of facets sharing an edge contain 3 common vertices.)

This covers all nodes in (26) except  $B$ . Here are the 4 incidences around  $B$ :

$$\begin{array}{ccccc} & & \sigma E_k & & \\ & & \parallel & & \\ & & \{m_{++}, m_{+-}, a_{k+1}, \sigma(a_k)\} & & \\ & & | & & \\ C_k & & B & & \epsilon_2 B \\ \parallel & \text{---} & \parallel & \text{---} & \parallel \\ \{m_{++}, p_+, a_k, a_{k+1}\} & & \{m_{++}, m_{+-}, p_+, a_{k+1}\} & & \{m_{++}, m_{+-}, p_+, \epsilon_2 a_{k+1}\} \\ & & | & & \\ & & \epsilon_4 C_k & & \\ & & \parallel & & \\ & & \{m_{+-}, p_+, a_{k+1}, a_k\} & & \end{array}$$

Hence we have checked that every facet appearing in Proposition 3.9 is incident to four facets, which are also  $\Gamma^+$ -conjugates of facets on our list. Hence our list of facets is complete.  $\square$

Below it will be useful to know the full incidence graphs of facets in a fundamental domain, as well as their incidences to facets which share a ridge with a facet in the fundamental domain. That is, are “just outside” the fundamental domain. Combining all incidences discovered in the previous proof, we obtain the following

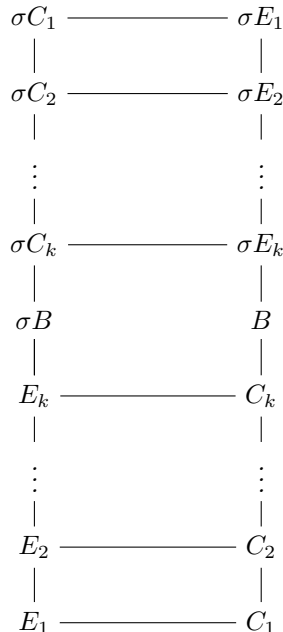
graph of incidences:

$$\begin{array}{ccccccc}
 & & & & \sigma E_k & & \\
 & & & & | & & \\
 & & & & B & \text{---} & \epsilon_2 B \\
 & & \sigma B & & | & \text{---} & \\
 & & | & & C_k & \text{---} & \epsilon_4 C_k \\
 \epsilon_3 C_k & \text{---} & E_k & \text{---} & C_k & \text{---} & \epsilon_4 C_k \\
 & & | & & | & & \\
 \epsilon_3 C_{k-1} & \text{---} & E_{k-1} & \text{---} & C_{k-1} & \text{---} & \epsilon_4 C_{k-1} \\
 & & | & & | & & \\
 & & \vdots & & \vdots & & \\
 & & | & & | & & \\
 \epsilon_3 C_2 & \text{---} & E_2 & \text{---} & C_2 & \text{---} & \epsilon_4 C_2 \\
 & & | & & | & & \\
 \epsilon_3 C_1 & \text{---} & E_1 & \text{---} & C_1 & \text{---} & \epsilon_4 C_1 \\
 & & | & & | & & \\
 & & \epsilon_2 E_1 & & \epsilon_2 C_1 & & 
 \end{array}
 \tag{27}$$

Note that every facet in our fundamental domain (i.e.  $B$ ,  $C_i$  and  $E_i$ ) is incident to 4 other facets, and so we know this graph describes all incidences amongst facets, one of which is in the fundamental domain. (We do not need incidences between facets not in the fundamental domain and have not included them above.)

**3.5. Quotients by sign flips.** Consider the facet-ridge graph of  $D_k^+$ . This is big and complicated. However, if we quotient by  $\Gamma^+$  we get something rather simple, as can easily be seen using the computations of the previous section. Sadly, this quotient is too coarse, and we lose too much information. However, by quotienting by the subgroup of  $\Gamma^+$  generated by sign flips we get a graph which is both easily visualized, and powerful enough to get bounds.

**Proposition 3.11.** *The quotient of the facet-ridge graph of  $D_k^+$  by the action induced by sign flips yields the following graph:*



(We ignore multiple edges and loops.)

*Proof.* Note that  $\Gamma^+$  is isomorphic to a the semi-direct product of the subgroup of sign flips and  $\langle \sigma \rangle$ . In particular, by Proposition 3.9 any facet is of the form  $\varepsilon \sigma^j Y$  where  $Y$  is one of the facets  $B, C_i$  or  $F_i, j \in \{0, 1\}$  and  $\varepsilon$  is a product of sign flips. In particular, our graph contains representatives of all orbits under sign flips. It is now a simple matter to unpack the incidences listed in the proof of Proposition 3.9 (or check the pictures on the previous page) to obtain the above graph.  $\square$

Actually, we need to consider a finer graph, which will almost certainly appear unmotivated at present. We ask for a few pages' worth of patience from the reader, where the relevance of this graph will become apparent.

Consider the face graph  $\Delta(D_k^+)$ . We define  $\tilde{\mathcal{G}}$  to be the full subgraph of  $\Delta(D_k^+)$  with nodes corresponding to the following faces of  $\Delta(D_k^+)$ :

- (1) All faces of dimension  $\geq 2$ ;
- (2) All edges of the form  $\{a_i, a_{i+1}\}$  and their  $\Gamma^+$ -orbits.
- (3) Four vertices given by the  $\Gamma^+$ -orbit of  $a_1$ .

We define  $\mathcal{G}$  to be quotient of  $\tilde{\mathcal{G}}$  by the action of sign flips.

**Proposition 3.12.** *The graph  $\mathcal{G}$  is isomorphic to the graph displayed in Figure 5.*

*Remark 3.13.* In Figure 5 we indicate the dimension of the face by colouring the node: black nodes are of dimension 3, blue nodes are of dimension 2, green nodes are of dimension 1 and the red nodes are of dimension 0.

*Proof.* We obtain the full subgraph of  $\mathcal{G}$  corresponding to faces of dimension  $\geq 2$  by taking the barycentric subdivision of the graph in Proposition 3.11. It remains

to fill in the faces of dimensions 0 and 1 (the red and green nodes in Figure 5). However, this is easy:  $\{a_i, a_{i+1}\}$  (resp.  $\sigma\{a_i, a_{i+1}\}$ ) is incident only to  $C_i$  and  $E_i$  (resp.  $\sigma(C_i)$  and  $\sigma(E_i)$ ) by inspection. Similarly,  $a_1$  is only incident to  $\{a_1, a_2\}$  and  $\sigma a_1$  is only incident to  $\sigma\{a_1, a_2\}$  and we're done.  $\square$

The following bound is critical to our main theorem. Its proof is by inspection of Figure 5:

**Corollary 3.14.** *For any  $F \in \{B, \sigma B, E_i, C_i\}$  we have*

$$\text{dist}_{\mathcal{G}}(F, \sigma a_1) \geq 2k + 3.$$

*Similarly, for any  $F \in \{B, \sigma B, \sigma E_i, \sigma C_i\}$  we have*

$$\text{dist}_{\mathcal{G}}(F, a_1) \geq 2k + 3.$$

**3.6. The pair embedding.** Now we focus on  $D = D_k$  with  $k \geq 1$  as above.

Recall the full subgraphs  $\Delta_D(D^-) \subset \Delta(D^-)$  and  $\Delta_D(D^+) \subset \Delta(D^+)$  defined in §2.3: they consists of facets which occur as the intersection of any face of  $F$  with the bottom (resp. top) drum skin. We would like to describe  $\Delta_D(D^-)$  and  $\Delta_D(D^+)$ . This is tricky, but it turns out that we can describe a graph which is (potentially) slightly bigger than  $\Delta_D(D^-)$ , but is small enough to estimate distances.

The bottom and top drum skins are isomorphic (via  $\tau$ ). However, there are many possible isomorphisms. We make the fixed and arbitrary choice to use  $\tau$  to identify the top and bottom drum skins. We will use superscript to indicate application of  $\tau$ . This applies to any face of  $D_k^+$ . So for example

$$a_1^- = \tau(a_1) \quad \text{and} \quad C_i^- = \tau(C_i).$$

*Remark 3.15.* This identification of vertices in the top and bottom drum skin is achieved in the colab [Co] `permute_axes()`. Be careful that one should only use this function to identify vertices in the top of drum skin with those in the bottom, and not vice versa! The identification of facets in the top and bottom drum skin is achieved using the dictionary `top_to_bottom_dict`.

Below a crucial role will be played by  $\sigma(a_1)$  (the ‘‘north pole’’ in Figure 5). To simplify notation we denote this point by  $n$ :

$$n = \sigma(a_1) = (0, 100, 0, 0, 1).$$

Similarly

$$n^- = \tau(n) = (0, 0, 0, 100, -1)$$

is the corresponding point in the bottom drum skin. We have:

**Theorem 3.16.** *The facet-vertex map is given on the top drum skin as follows:*

$$\phi^+(B) = a_1^-, \quad \phi^+(C_i) = n^- \quad \text{and} \quad \phi^+(E_i) = n^-.$$

*On the bottom drum skin it is given by*

$$\phi^-(B^-) = n, \quad \phi^-(C_i^-) = a_1 \quad \text{and} \quad \phi^-(E_i^-) = a_1$$

*Remark 3.17.* If we had to try to isolate one key fact that makes our examples work, it would be Theorem 3.16.

*Remark 3.18.* As pointed out by a referee, the “double pancake” structure remarked upon in Remark 3.8 goes some way to explaining the simple form of the facet vertex map in Theorem 3.16. Indeed, consider a polytope  ${}_\varepsilon D_k^+$  obtained by multiplying the first two coordinates by  $\varepsilon$ , where  $\varepsilon$  is roughly  $1/50$ . Then  ${}_\varepsilon D_k^+$  is combinatorially equivalent to  $D_k^+$ , and the coordinates of its vertices are all of a similar order of magnitude. Thus, we expect the directions of the normals to facets to be reasonably well-distributed on the 3-sphere. However, as  $\varepsilon \rightarrow 1$  the first two coordinates are scaled rather drastically, and these normal vectors approach the unit circle in the 3-sphere spanned by the last two coordinates. This explains why only the “extremal” vertices occur in the image of the facet vertex map in Theorem 3.16. This scaling technique was observed (and used for a similar purpose) in [MSW15, Lemma 2.13].

*Remark 3.19.* The reader wishing to witness this little miracle in the colab [Co] should see the cells labelled **Facet-vertex map for top facets** for  $\phi^+(B)$ ,  $\phi^+(C_i)$  and  $\phi^+(E_i)$  and **Facet-vertex map for bottom facets** for  $\phi^-(B^-)$ ,  $\phi^-(C_i^-)$  and  $\phi^-(E_i^-)$ .

*Proof.* We will use knowledge obtained in the course of the proof of Proposition 3.9. As in that proof, we proceed facet by facet.

We will make essential use of the method outlined in §2.4 to determine the facet-vertex map.

*Facet B:* We have in the proof of Proposition 3.9 that

$$f_B = \left(-1, -\frac{24}{25}, -49, 0, 3 \cdot 49\right)$$

yields a functional which cuts out  $B$  from our top drum skin. By Lemma 2.7, in order to determine  $\phi^+(B)$ , we only need to determine the vertex  $v$  in the bottom drum skin on which  $f_B$  takes its minimum. By inspection, this occurs at

$$v = (0, 0, 100, 0).$$

That is,  $\phi^+(B) = a_1^-$  as claimed.

*Facet  $E_i$ :* As in the proof of Proposition 3.9 for  $E_i$ , let us split  $\mathbb{R}^4 = \mathbb{R}^2 \oplus \mathbb{R}^2$  and consider the same functional  $f = f_1 + f_2 + 1$  as there. Note that

$$f_1((75, 75)) \geq -1$$

and hence (using that  $f_1$  is  $-1$  on  $a_i$  and  $a_{i+1}$ ) that

$$(28) \quad f_1(v) \geq -1/25 \quad \text{for } v = (\pm 3, \pm 3), (\pm 1, 0) \text{ or } (0, \pm 1)$$

$$(29) \quad f_1((1, 0)) \geq -1/75.$$

Also, we have  $f_2((c, d)) = -\frac{1}{3}d$ . Using this explicit form of  $f_2$  and (28) it is clear that  $f$  takes its minimum value at either

$$(0, 0, 0, 100) \quad \text{or} \quad (1, 0, 0, 98).$$

Now  $-100/3 < -98/3 - 1/75$  and hence  $f$  takes its minimum of the first point, i.e.  $n^-$ . Thus  $\phi^+(E_i) = n^-$  as claimed.

*Facet  $C_i$ :* Again, we make crucial use of knowledge gleaned in the course of the proof of Proposition 3.9. We decompose  $f = f_1 + f_2 + 1$  as in Proposition 3.9. We saw there that

$$(30) \quad f_2 = (\delta_2, -\frac{1}{3} - \delta_2).$$

where  $\delta_2$  satisfies

$$-0.04 < \delta_2 \leq -0.02$$

From the form of  $f_2$  it follows that amongst the  $\Gamma^+$  orbits of  $\{a_i^-\}$ ,  $f$  takes its minimum value at  $n^-$ . It is also clear that amongst the  $\Gamma^+$ -orbits of  $p_+^-$ ,  $f$  takes its minimum value at  $(1, 0, 0, 98)$ . Finally, we claim that

$$f((0, 0, 0, 100)) < f((1, 0, 0, 98)).$$

Expanding and rearranging, we see that this is true if and only if we have the inequality:

$$2 \cdot f_2((0, 1)) < f_1((1, 0)).$$

By (15) we have  $f_1((1, 0)) > -\frac{1}{100}$ , and by (30) we have  $f_2((0, 1)) = -\frac{1}{3} - \delta_2$ . Thus the inequality holds, and we have  $\phi^+(C_i) = n^-$  as claimed.

This completes the proof of Theorem 3.16 for facets  $B$ ,  $C_i$  and  $E_i$  in the top drum skin.

For those in the bottom drum skin we employ a symmetry argument. Because  $\phi^+(B) = a_1^-$  there exists a facet  $F$  of the drum  $D_k$  incident to both  $B$  and  $a_1^-$ . Acting by  $\tau$  we see that there is a facet  $\tau(F)$ , incident to both  $B^-$  and  $\tau(a_1^-) = \tau^2(a_1) = \sigma(a_1) = n$ . This proves that  $\phi^-(B^-) = n$  as claimed. The statements  $\phi^-(C_i^-) = \phi^-(E_i^-) = \tau(n^-) = \tau^2(n) = \sigma(n) = a_1$  follows by the same argument. The theorem is proved.  $\square$

In order to establish our main theorem, we need to know a little more about the pair embedding:

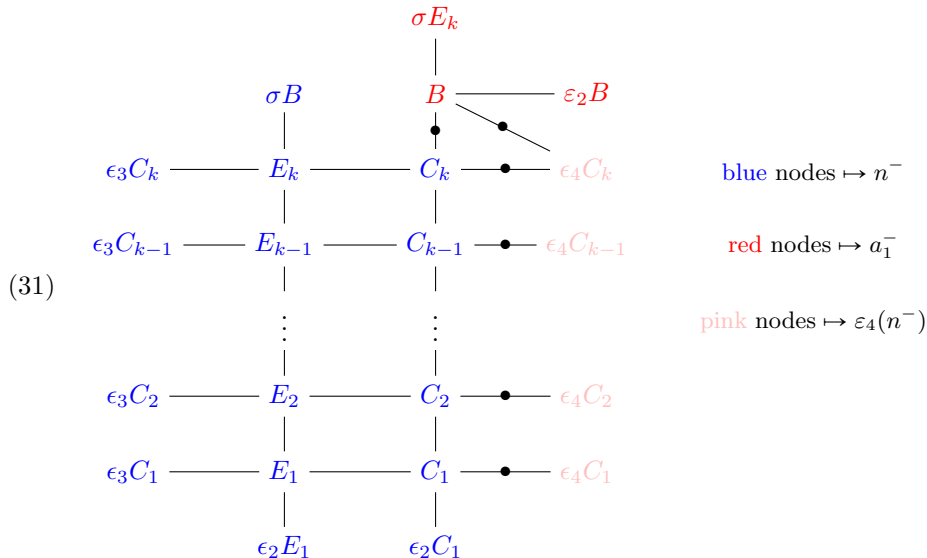
**Theorem 3.20.** *Only boundary edges occur in the image of the pair embedding. More precisely, suppose that  $E$  is an edge of  $D_k^-$  and that  $\rho(F) = (X, E)$  for some facet  $F$  of  $D_k$ . Then  $E$  belongs to the  $\Gamma^+$ -orbit of  $\{a_i^-, a_{i+1}^-\}$  for some  $i$ .*

The next section is devoted to the proof.

**3.7. The pair embedding II.** Consider the incidence graph of facets incident to the fundamental domain in (27). Using Theorem 3.16 and the fact that the facet-vertex map is equivariant one computes easily that the images of the facets displayed in



(27) are given as follows:



More precisely, the images of  $B, C_i$  and  $E_i$  are read off directly from Theorem 3.16. To compute the remaining images one uses equivariance. For example,  $C_k$  maps to  $n^-$  by Theorem 3.16 and hence  $\epsilon_4 C_k$  maps to  $\epsilon_4(n^-)$ .

Recall that edges in the above graph correspond to certain ridges in  $D_k^+$ . We have indicated edges where the facet-vertex map takes different values at the facets corresponding to the end points by adding a bullet to the edge. We can then apply Corollary 2.10 to deduce that we only need to determine the facet-ridge map for facets in the full drum which involve these ridges.

We handle these ridges one at a time:

*Ridge*  $R = B \cap C_k$ :

We apply Lemma 2.9 with a minor variation. We determine all functionals which are zero on  $R$  and  $< 0$  on  $D_k^+ - R$  and we compute their maxima on  $D_k^-$ . (We have switched  $\geq 0 \leftrightarrow \leq 0$  and maxima  $\leftrightarrow$  minima with respect to Lemma 2.9. This simplifies some of the constants below.) It is enough to show that all maxima are in the  $\Gamma^+$ -orbit of  $a_i^-$ . (We use that the only edges involving only the  $a_i^-$  are  $\Gamma^+$ -orbits of edges of the form  $(a_i^-, a_{i+1}^-)$ . This is an easy consequence of symmetry and Proposition 3.9.)

Consider the functional given by

$$f = (x_1, x_2, x_3, x_4, x_5) \quad \text{i.e.} \quad f((v_1, \dots, v_4)) = \sum x_i v_i + v_5.$$

We now determine the conditions for  $f$  to vanish on our ridge  $R$  and be  $\leq 0$  on  $D_k^+$ . Certainly,  $x_5 \neq 0$  as  $D_k^+$  contains 0 in its interior. Hence we may assume that

$$(32) \quad x_5 = -150.$$

Now  $f$  vanishes at  $a_{k+1}$  and is  $\leq 0$  on the  $\Gamma^+$ -orbit of the  $a_i$ . Writing out what that means for  $a_{k+1}$  and the  $\Gamma^+$  orbit of  $a_1$  we deduce the inequalities

$$(33) \quad x_1 + x_2 = 2 \quad \text{and} \quad \frac{1}{2} \leq x_i \leq \frac{3}{2} \quad \text{for } i = 1, 2.$$

Because  $f$  vanishes at  $m_{++}$  and is  $\leq 0$  on  $m_{\pm\pm}$  we deduce that

$$(34) \quad x_3 + x_4 = 50, \quad x_3, x_4 \geq 0.$$

Finally, because  $f$  takes the value 0 at  $p_+$  and is  $< 0$  at  $\sigma(p_+)$  we deduce that

$$(35) \quad x_3 = 150 - 98x_1 \quad \text{and} \quad x_4 < 150 - 98x_2.$$

Combining (35), (34) and (33) we deduce that

$$(36) \quad \frac{50}{49} \leq x_1 \leq \frac{3}{2}, \quad \frac{1}{2} \leq x_2 \leq \frac{48}{49}, \quad 3 \leq x_3 \leq 50.$$

It remains to compute the maximum of  $f$  on  $D_k^-$ .

We will now show that  $f$  obtains its maximum on the  $\Gamma^+$ -orbit of some  $a_i^-$ . In order to do this, it is enough to show that  $f$  obtains its maximum neither on the  $\Gamma^+$ -orbit of  $m_{\pm\pm}$  nor the orbit of  $p_{\pm}^-$ . Firstly note that on each orbit it takes its maximum value on vectors all of whose coordinates are positive, i.e.  $m_{++}^-$  or  $p_+^-$  and  $\sigma(p_+^-)$  respectively.

Now, at  $m_{++}^-$ ,  $f$  takes the value  $3(x_1 + x_2) = 6$ , which is much less than its value at  $a_k = 50 \cdot 75$ .

It is slightly more subtle to see the statement for the  $p_+^-$  and  $\sigma(p_+^-)$ . Firstly, suppose that  $x_3 \geq x_4$ . Then  $x_3$  is at least 25 by (34) and hence

$$f(\sigma(p_+)^-) \leq f(p_+^-) = x_2 + 98x_3 < 100x_3 = f(a_1^-).$$

Hence in this case neither  $f(p_+^-)$  nor  $f(\sigma(p_+)^-)$  is maximal. On the other hand, if  $x_3 \leq x_4$  then  $x_4$  is at least 25 and

$$f(p_+^-) \leq f(\sigma(p_+)^-) = x_1 + 98x_4 < 100x_4 = f(n^-).$$

Hence in this case, again neither  $f(p_+^-)$  nor  $f(\sigma(p_+)^-)$  is maximal. This completes the proof.

*Ridge  $R = B \cap \varepsilon_4 C_k$ :* We can handle this by symmetry:  $\varepsilon_4$  fixes  $B$  and sends  $C_k$  to  $\varepsilon_4 C_k$ . Thus this case follows from the previous one, as  $\varepsilon_4$  permutes boundary edges.

*Ridge  $R = C_i \cap \varepsilon_4 C_i$ :* The ridge  $R$  has vertices  $a_i, a_{i+1}$  and  $p_+$ . We use the same method as in the first case handled above: first we write down conditions satisfied by all functionals which are  $= 0$  on  $R$  and  $< 0$  on  $D_k^+ - R$ , and then show that the maxima on  $D_k^-$  is contained in a boundary vertex or edge.

As before consider the functional

$$f = (x_1, x_2, x_3, x_4, x_5) \quad \text{i.e.} \quad f((v_1, \dots, v_4)) = \sum x_i v_i + v_5.$$

and assume that  $f$  is  $= 0$  on  $R$  and  $< 0$  on  $D_k^+ - R$ . Certainly  $x_5 \neq 0$  as 0 is in the interior of  $D_k^+$  and we can (and do) assume that

$$(37) \quad x_5 = -102.$$

The equation  $x_1 u + x_2 v - 102$  (the restriction of our functional to the span of the first two coordinates) determines a functional which vanishes on the two points  $a_i$  and  $a_{i+1}$ . We deduce that the  $u$ - (resp.  $v$ -) intercept is given by

$$u = 102/x_1 \quad \text{resp.} \quad v = 102/x_2.$$

Our assumptions (15) and (16) then imply that

$$(38) \quad 1 \leq x_1 \leq \frac{102}{100} = 1.02$$

and

$$(39) \quad 0 < x_2 < 102/283 \approx 0.36.$$

Because our function vanishes on  $p_+$  we have

$$(40) \quad x_3 = 102 - 98x_1 \quad \text{and thus} \quad 2.04 < x_3 \leq 4.$$

We already have enough to deduce what we need: (38), (39) and (40) are enough to deduce that amongst the points  $m_{\pm, \pm}^-$ ,  $p_{\pm}^-$  and  $a_i^-$  our functional  $f$  obtains its maximum at the orbit of one of the  $a_i^-$ , which is what we were hoping to prove.

*Remark 3.21.* With a little more care, one can establish that in the case of the ridge  $B \cap C_k$ , all points

$$a_1^-, a_2^-, \dots, a_{k-1}^-, a_k^-, \sigma(a_k^-), \dots, \sigma(a_2^-), \sigma(a_1^-)$$

can be obtained as maxima of a suitable  $f$ .

Similarly, one can also see that in case of the ridge  $R = B \cap \varepsilon_4 C_i$  all points

$$-\sigma(a_1^-), -\sigma(a_2^-), \dots, -a_2^-, a_1^-, a_2^-, \dots, a_{k-1}^-, a_k^-, \sigma(a_k^-), \dots, \sigma(a_2^-), \sigma(a_1^-)$$

can be obtained as maxima of a suitable  $f$ .

One can see an illustration of this phenomenon in the colab [Co] in the cell: **Edges incident to a fixed ridge in the top drum skin.**

**3.8. Proof of our main theorem.** We now have all the pieces in place to explain our proof of Theorem 1.1.

As explained in §2.3, a priori we need to compute the distance between the top and bottom drum skin in the facet ridge graph  $\mathcal{F}(D_k)$ . Instead, we can compute distances in the trimmed facet ridge graph  $\mathcal{F}^t(D_k)$ . In order to do this we can try to use the pair embedding

$$\mathcal{F}^t(D_k) \hookrightarrow \Delta(D^-) \times \Delta(D^+).$$

Unfortunately, the bounds we get in this way are not strong enough.

Recall the graphs  $\tilde{\mathcal{G}}$  and  $\mathcal{G}$  introduced in § 3.5. We let  $\tilde{\mathcal{G}}^-$  and  $\mathcal{G}^-$  denote their obvious analogues for the bottom drum skins. By Theorems 3.16 and 3.20 the only 0 and 1-dimensional facets in the image of the pair embedding are the  $\Gamma$  orbits of the point  $a_1$  and the edges  $\{a_i, a_{i+1}\}$ . Thus, by definition of  $\tilde{\mathcal{G}}$  and  $\tilde{\mathcal{G}}^-$  we instead obtain an embedding

$$\mathcal{F}^t(D_k) \hookrightarrow \tilde{\mathcal{G}}^- \times \tilde{\mathcal{G}}.$$

Quotienting by sign flips we obtain an embedding

$$(41) \quad \mathcal{F}^t(D_k)/\text{sign flips} \hookrightarrow \mathcal{G}^- \times \mathcal{G}.$$

Finally, note that by Corollary 3.14 we have the following bounds on distances in  $\mathcal{G}$ :

$$(42) \quad \text{dist}_{\mathcal{G}}(B, n) \geq 2k + 3,$$

$$(43) \quad \text{dist}_{\mathcal{G}}(B, a_1) \geq 2k + 3,$$

$$(44) \quad \text{dist}_{\mathcal{G}}(X, n) \geq 2k + 3 \quad \text{for any } X \in \{C_i, E_i\}.$$

We also have analogues of the above for  $\mathcal{G}^-$ , for example  $\text{dist}_{\mathcal{G}^-}(B^-, n^-) \geq 2k + 3$ .

**Theorem 3.22.**  $D_k$  has width  $\geq 5 + k$ .

In the proof, the facets  $B$  and  $\{C_i, E_i\}$  play very different roles. In order to lighten notation, we use  $X^-$  (resp.  $X$ ) to denote any element of the set  $\{C_i^-, E_i^-\}$  (resp.  $\{C_i, E_i\}$ ).

*Proof.* Our drum  $D_k$  has width  $\geq 5 + k$  if and only if any path  $F_0, F_1, \dots, F_\ell$  of facets in the trimmed facet ridge graph of  $D_k$  has length (see (5)):

$$(45) \quad \ell \geq 3 + k$$

For the rest of the proof we will use the pair embedding to regard each  $F_i$  as a pair of faces in the top and bottom drum skin. We further pass to the quotient by sign flips and regard facets as pairs of nodes in  $\mathcal{G}^- \times \mathcal{G}$  via (41). Using the symmetry  $\sigma$  of  $\mathcal{G}^-$  we can additionally assume that that  $(F_0)_{\text{bot}}$  is either  $B^-$  or  $X^-$  (see Proposition 3.9). We analyse these cases separately:

*Case 1:*  $(F_0)_{\text{bot}} = B^-$ . By Theorem 3.16 we must have

$$F_0 = (B^-, n).$$

Applying Theorem 3.16 again, we conclude that either

$$F_\ell = (n^-, X) \quad \text{or} \quad F_\ell = (a_1^-, \sigma(B)).$$

If  $F_\ell = (n^-, X)$  then we have

$$\text{dist}(F_0, F_\ell) \geq \frac{1}{2}(\text{dist}_{\mathcal{G}}(B^-, n^-) + \text{dist}_{\mathcal{G}}(n, X)) \stackrel{(42)}{\geq} \frac{1}{2}((2k+3) + 3) = k+3$$

where the first inequality is a consequence of Proposition 2.3.

If  $F_\ell = (a_1^-, \sigma(B))$  then we have

$$\text{dist}(F_0, F_\ell) \geq \frac{1}{2}(\text{dist}_{\mathcal{G}}(B^-, a_1^-) + \text{dist}_{\mathcal{G}}(n, \sigma(B))) \stackrel{(43)}{\geq} \frac{1}{2}((2k+3) + 3) = k+3$$

where again we use Proposition 2.3 for the first inequality.

*Case 2:*  $(F_0)_{\text{bot}} = X^-$ . By Theorem 3.16, we must have

$$F_0 = (X^-, a_1).$$

Applying Theorem 3.16 again, we also conclude that either

$$F_\ell = (n^-, X) \quad \text{or} \quad F_\ell = (a_1^-, \sigma(B)).$$

If  $F_\ell = (n^-, X)$  then we have

$$\text{dist}(F_0, F_\ell) \geq \frac{1}{2}(\text{dist}_{\mathcal{G}}(X^-, n^-) + \text{dist}_{\mathcal{G}}(a_1, X)) \stackrel{(44)}{\geq} \frac{1}{2}((2k+3) + 3) = k+3.$$

If  $F_\ell = (a_1^-, \sigma(B))$  then we have

$$\text{dist}(F_0, F_\ell) \geq \frac{1}{2}(\text{dist}_{\mathcal{G}}(X^-, a_1^-) + \text{dist}_{\mathcal{G}}(a_1, \sigma(B))) \geq \frac{1}{2}(3 + (2k+3)) = k+3$$

where, for the second inequality, we have used that

$$\text{dist}_{\mathcal{G}}(a_1, \sigma(B)) = \text{dist}_{\mathcal{G}}(n, B) \geq 2k+3$$

by symmetry and (42).

Thus we have established (45) in all cases, and the theorem is proved.  $\square$

## REFERENCES

- [Co] Colab for “Drums of High Width”.  
tiny.cc/1ioivz Accessed: 2023-12-15.
- [HW10] M. Heule and T. Walsh. Symmetry within solutions. In *Proceedings of AAAI*, volume 10, pages 77–82, 2010.
- [KW67] V. Klee and D. W. Walkup. The  $d$ -step conjecture for polyhedra of dimension  $d < 6$ . *Acta Math.*, 117:53–78, 1967.
- [MSW15] B. Matschke, F. Santos, and C. Weibel. The width of five-dimensional prisms. *Proc. Lond. Math. Soc. (3)*, 110(3):647–672, 2015.
- [San12] F. Santos. A counterexample to the Hirsch conjecture. *Ann. of Math. (2)*, 176(1):383–412, 2012.

GOOGLE DEEPMIND.  
Email address: `adavies@google.com`

GOOGLE DEEPMIND.  
Email address: `prateek.gupta@exeter.ox.ac.uk`

GOOGLE DEEPMIND.  
Email address: `sracaniere@google.com`

GOOGLE DEEPMIND.  
Email address: `swirszcz@google.com`

WORCESTER POLYTECHNIC INSTITUTE, USA.  
Email address: `zadam@wpi.edu`

GOOGLE DEEPMIND.  
Email address: `theophane@google.com`

UNIVERSITY OF SYDNEY, AUSTRALIA.  
Email address: `g.williamson@sydney.edu.au`

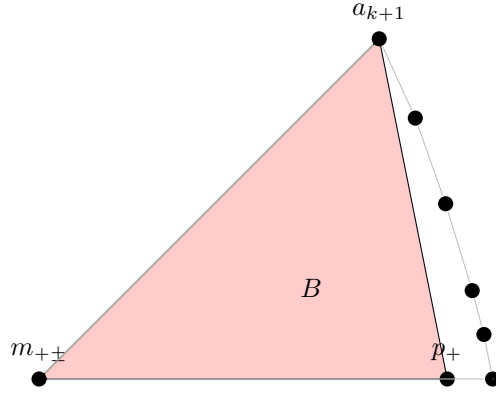
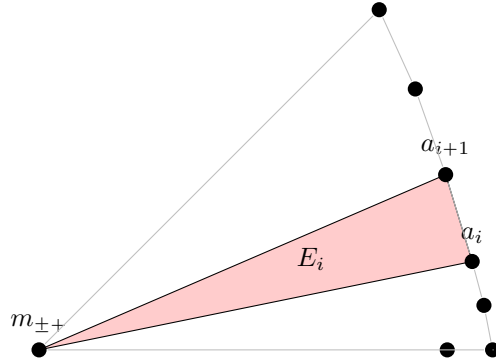
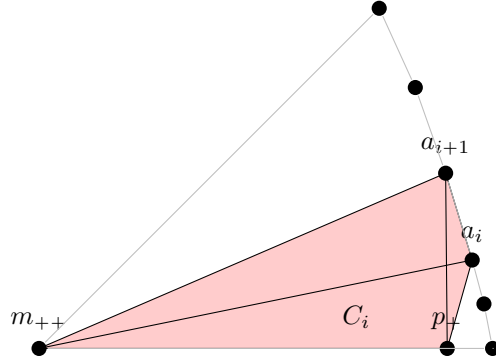
FIGURE 2. Projection of the facet  $B$ .FIGURE 3. Projection of the facet  $E_i$ .FIGURE 4. Projection of the facet  $C_i$ .

FIGURE 5. The subgraph  $\mathcal{G}$ .